Korean J. Chem. Eng., 32(11), 2319-2329 (2015)
DOI: 10.1007/s11814-015-0065-3

pISSN: 0256-1115
eISSN: 1975-7220

Preparation and characterization of PES/SiO_2 composite ultrafiltration membrane for advanced water treatment

Mimi Suliza Muhamad*,†, Mohamad Razman Salim*,†, and Woei-Jye Lau**

*Centre for Environmental Sustainability and Water Security (IPASA), Research Institute for Sustainable Environment (RISE), Faculty of Civil Engineering, Universiti Teknologi Malaysia, 81310 Skudai, Johor, Malaysia
**Advanced Membrane Technology Research Centre (AMTEC), Universiti Teknologi Malaysia, 81310 Skudai, Johor, Malaysia
(*Received 2 February 2015 • accepted 1 April 2015*)

Abstract−Polyethersulfone (PES) is a commonly used polymeric material for the fabrication of ultrafiltration (UF) membranes. However, the hydrophobic nature of PES leads to poor membrane performance with low anti-fouling properties during filtration process. Hence, for this study, the PES-based hollow fiber membrane was modified with inorganic silicon dioxide (SiO_2) nanoparticles of various loading (from zero to 4 wt%), aiming to improve the membrane properties for advanced water treatment process. The characterization of the surface morphology, physical and chemical properties of novel PES/SiO_2 composite membranes was performed by SEM, FTIR-ATR, TGA and contact angle analyzer. The SEM images show the changes in membrane structure as well as skin layer thickness upon addition of SiO_2 nanoparticles. The FTIR-ATR analysis shows the functional group of SiO_2 in the polymer matrices. Results further show that the presence of 2 wt% SiO_2 in the membrane matrix is the best loading to improve the water flux and bovine serum albumin (BSA) rejection, achieving 87.2 L/m^2·h and 94%, respectively. As a comparison, the control PES membrane only exhibits water flux of 44.2 L/m^2·h and rejection of 81%. Results also show that the flux recovery percentage of the membrane was improved from 82% in the control membrane to 93% in the membrane incorporated with 2 wt% SiO_2, indicating improved membrane anti-fouling property. Furthermore, the PES/SiO_2 membrane shows huge potential for advanced water treatment, as the qualities of the permeate samples treated by this membrane could meet the limit set by a local water company.

Keywords: Polyethersulfone, Ultrafiltration, Silicon Dioxide, Advanced Water Treatment, Anti-fouling Performance

INTRODUCTION

Every day, hundreds-thousands gallons of water are consumed by the general population across the world to support daily life. Water can be considered as one of the most crucial elements for living things on earth and precious resource for human civilization [1]. Owing to the increasing world population over the past 50 years, there is a strong growing demand for the fresh water for daily consumption [2,3]. In view of this, the waterworks industries face major challenges to improve the efficiency and cost of water treatment process in order to overcome water shortages and produce clean and safe drinking water for public.

In recent years, membrane technology has emerged as one of the main solutions for problems relating to water [3]. The use of membranes for water treatment is increasingly important due to the water scarcity encountered by some countries and/or stringent regulations in industrialized countries [4]. The physical separation process of contaminants using membrane technology has been widely applied in many water and wastewater treatment processes. Some of its applications are the production of potable water from surface water/groundwater/brackish water [5-8] or recycling of industrial effluent for reuse purposes [3]. The effectiveness of membrane technology in removing a wide variety of water contaminants has increased the use of this process in water purification to replace or improve conventional treatments [9]. Membrane separation is one of the best options for drinking water treatment as the process does not utilize any chemicals [10]. Other advantages of using membrane process include small footprint, low energy cost, easy to use and high quality of permeate produced [11,12].

Ultrafiltration (UF) is the membrane technology that has been widely employed in water treatment. About 50% of the UF membrane plants are being used to treat river, reservoir, and lake waters [3]. This technology has been used in municipal drinking water application for more than 20 years [13]. It has been broadly utilized for drinking water treatment [14-16] and pre-treatment option for nanofiltration [17,18] or reverse osmosis process [19,20]. The application of hollow fiber UF membrane in treating river water for drinking water production has shown to be efficient in removing not only particles and bacteria but also other organic compounds present in the raw water [21,22]. Nevertheless, the problem of using membranes is the occurrence of fouling that causes the accumulation of materials on the surface or within the membrane, which consequently lead to reduction in the amount of filtered water over time [9]. Therefore, to maintain membrane performance efficiency over operation time, the membrane surface has to be modified.

The efficiency of UF membranes is dependent on the polymeric material that is used for membrane fabrication. Most of the polymeric-based membranes are made from synthetic organic poly-

†To whom correspondence should be addressed.
E-mail: msuliza@gmail.com, mohdrazman@utm.my

mers such as cellulose acetate (CA), polysulfone (PS), polyethersulfone (PES), polyacrylonitrile (PAN), polyvinylidene fluoride (PVDF), polyvinyl alcohol (PVA) and polyimide (PI) [23,24]. Among these materials, PES is the most commonly used for UF membrane making, as it provides high mechanical, thermal (up to 50 °C) and chemical resistances. Moreover, PES has reasonable pH tolerances (4-10), good chlorine resistance and high flexibility in membrane fabrication [25,26]. However, PES has low hydrophilic property, which makes it prone to fouling problems [24]. The occurrence of membrane fouling during filtration will lead to reduction of water flux and might affect water quality produced [27]. To overcome the problem, many types of organic and inorganic additives can be used to improve the properties of the PES-based membrane.

Current research that focuses on membrane surface modification is to incorporate nanoparticles into polymeric membranes. The aim of introducing nanoparticles to membrane matrix is to improve not only membrane surface hydrophilicity but also other characteristics such as separation performance, antifouling resistance, and mechanical properties [24,28,29]. Previous work has indicated that hydrophilicity is one of the most important properties that can affect water flux, solute rejection and fouling resistance of a membrane [30]. The nanoparticles that have been used to increase membrane hydrophilicity include silver nitrate ($AgNO_3$) [31], aluminium oxide (Al_3O_2) [32], zirconium oxide (ZrO_2) [33], titanium oxide (TiO_2) [34], lithium bromide (LiBr) [35] and silicon dioxide (also known as silica) (SiO_2) [36]. For drinking water application, SiO_2 nanoparticles are more suitable to be incorporated into the membranes because SiO_2 exhibits lower toxicity compared to other nanoparticles and is also environmentally inert [28]. In addition, SiO_2 has been previously reported to be important in improving membrane anti-fouling property [37-40].

There are many ways of incorporating nanoparticles into the polymeric solution. One is by direct blending the SiO_2 nanoparticles into the PES dope solution and stirring for a while to obtain a homogeneous solution [41]. However, direct use of SiO_2 nanoparticles will cause them to agglomerate easily and not disperse well in the dope solution. Therefore, surface modification of nanoparticles by surfactant is necessary. One commonly used surfactant is sodium dodecyl sulfate (SDS). The amphiphilic character of surfactants allows for self-association or micellization in solution [42]. The formed SDS micelles will attach to the individual SiO_2 nanoparticle and prevent it from agglomerating with other nanoparticles. This, as a result, reduces agglomeration of nanoparticles in dope solution and further improves their distribution in membrane matrix. In this study, hollow fiber composite membranes made of different SiO_2 contents were prepared by phase inversion (dry/wet spinning) method and applied as an advanced water treatment for drinking water. The morphology of the membranes was characterized by scanning electron microscope (SEM), while the surface functionalization of SiO_2 was examined by Fourier transform infrared spectroscope (FTIR). The thermal properties and surface hydrophilicity of membranes was characterized using thermogravimetric analyzer (TGA) and contact angle goniometer, respectively. The effects of modified SiO_2 nanoparticles on the UF performances, hydrophilicity, anti-fouling performance and application as an advanced treatment for drinking water were discussed.

EXPERIMENTAL

1. Materials

PES polymer (Radel® A) with specific gravity of 1.37 purchased from Solvay Specialty Polymers, USA was used as the main membrane material. SiO_2 nanoparticles (average particle size of 10-20 nm) were used as inorganic additives. Sodium dodecyl sulfate (SDS) was used to modify SiO_2 nanoparticles by minimizing the agglomeration of the nanoparticles. Polyvinylpyrrolidone (PVP, Mw: 40 g/mol) was used as pore former agents and N,N-dimethylacetamide (DMAc) as solvent. Bovine serum albumin (BSA, Mw: 67 g/mol) and PVP (Mw: 10, 40 and 360 g/mol) were used for solute rejection tests. All of these chemicals were supplied by Sigma Aldrich, USA. The chemical structure of PES, SDS, PVP and SiO_2 are illustrated in Fig. 1.

2. Water Sampling and Characterization

Water sampling was conducted at Water Treatment Plant (WTP) of Sungai Skudai, Johor Bahru, Malaysia. Since the membranes of this work were fabricated for advanced treatment processes, the

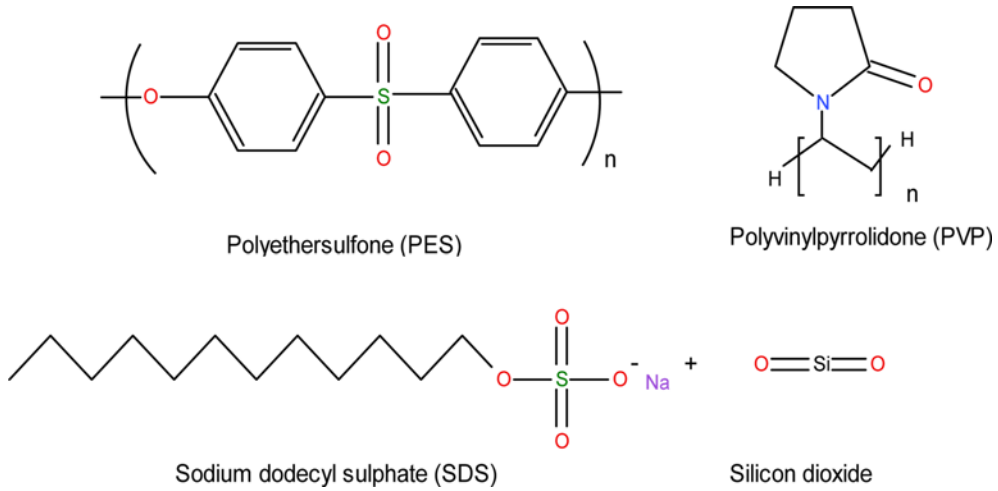

Fig. 1. Chemical structures of PES, PVP, SDS and SiO_2.

water sample was collected from the filtration tank of the treatment plant where the water was pre-treated by screening, flocculation/coagulation and sedimentation. The water samples were characterized with respect to pH, dissolved oxygen (DO), and temperature using pH-DO portable meter (Orion 4 star, Thermo Scientific). Turbidity was measured with a portable turbidimeter (2100Q, Hach). Total organic carbon (TOC) and dissolved organic carbon (DOC) were measured using total organic carbon analyzer (TOC-LCPN, Shimadzu). Chemical oxygen demand (COD), ammonia nitrogen, ferum, aluminium and manganese were measured by UV-vis spectrophotometer (DR5000, Hach). All these analytical methods used in this study were based on APHA Standard Method. The bacterial count in the water sample before and after PES/SiO_2 membrane filtration process was performed by spreading plate of water samples into the nutrient agar (NA) culture medium. The plates were incubated at 37 °C for 24 h and the numbers of colonies form on the plates were determined by the plate count method.

3. Membrane Preparation

First, the SiO_2 nanoparticles were modified using SDS solution according to a previous work [36]. In the modification process, 3.5 vol% SDS solutions was prepared in 1,000 mL deionized water. Then, 5.0 g SiO_2 was added to the solution and the pH was adjusted to 4 using H_2SO_4. The solution was vigorously stirred for 8 h, then centrifuged and filtered to obtain the white SiO_2 nanoparticles. Fig. 2 illustrates the reaction mechanism between SiO_2 and SDS. For dope solution preparation, 18 wt% PES pellets were added into preweighed DMAc solvent. After that, the solution was stirred at 600 rpm until all the PES pellets were completely dissolved. The process was followed by addition of 6 wt% PVP and SiO_2 nanoparticles of various loading (0, 1, 2 or 4 wt%). The dope solution was then ultrasonic-vibrated for 30 min to remove air bubbles within the solution and to ensure good dispersion of the particles prior to spinning process.

The PES/SiO_2 composite membranes were prepared by phase inversions method. Dry/wet spinning method with air gap of 10 cm was employed to fabricate hollow fiber membranes containing different amount of SiO_2 nanoparticles. The non-solvent used as bore fluid was deionized water, while external coagulation bath was tap water at 25±1 °C. The ratio of dope flow rate to bore fluid flow rate was kept constant for all membranes. During spinning process, the dope solution and bore fluid was passed through a spinneret with 1.25/0.55 mm orifice outer/inner diameter at the pressure of N_2 and constant-flow pump. The dope solution was pressurized through spinneret with controlled dope extrusion rate of 3 mL/min, while the internal coagulant was kept at 1.8 mL/min. The hollow fiber that emerged from the tip of the spinneret was guided through the two water baths at a take up velocity of 15.7 cm/s before being collected by a wind-up drum. The spun hollow fibers were stored in the water bath for 24 h to remove the residual DMAc and the PVP additives.

The hollow fibers were then post-treated using glycerol:water (10 : 90) solution for another 24 h to minimize fiber shrinkage and pore collapse during air-drying. Composition and the spinning conditions of the fabricated hollow fiber PES membranes are summarized in Table 1. Prior to membrane module preparation, the fibers were air-dried at room temperature for 3 days. A bundle of 10 hollow fibers with approximate length of 20 cm was potted into stainless steel adapter using epoxy resin (E-30CL Loctite® Corporation, USA) to form a module. The module was then left at room temperature for hardening before being put into stainless steel hous-

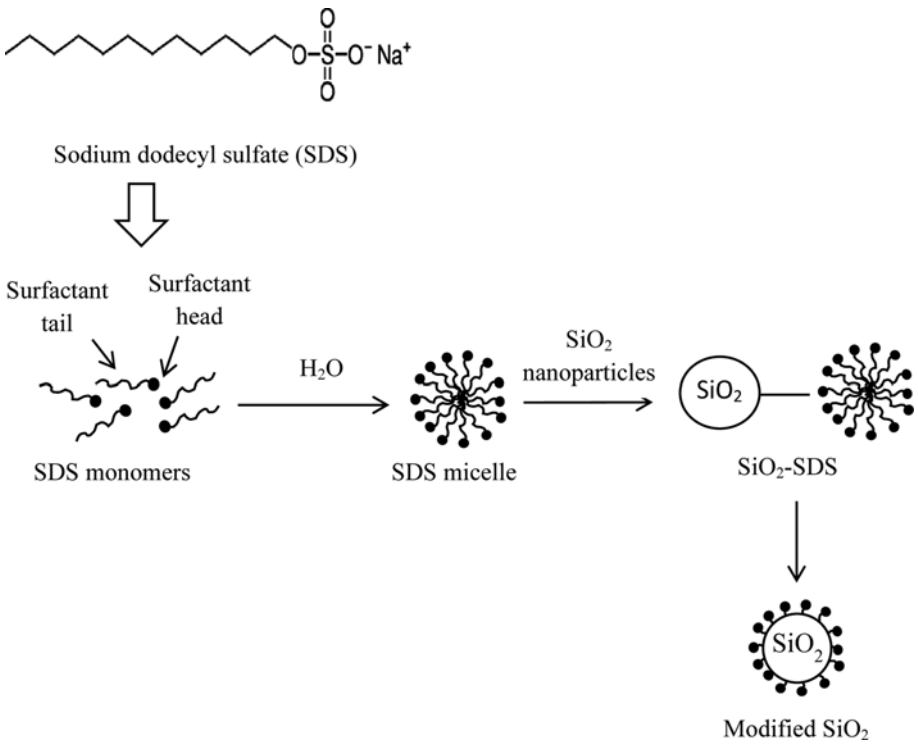

Fig. 2. Reaction mechanism of SiO_2 with SDS.

Table 1. Spinning parameters of PES/SiO_2 hollow fiber membranes

Spinning parameter	Values
Dope composition (PES/PVP/SiO_2/DMAc)	(18/6/0/76), (18/6/1/75), (18/6/2/74), (18/6/4/72)
Nitrogen extrusion pressure	1-1.5 psi
Dope extrusion rate	3.0 cm^3/min
Spinneret OD/ID	1.25 mm/0.55 mm
Bore fluid flow rate	1.8 cm^3/min
Bore fluid	Deionized water
External coagulant bath	Tap water
External coagulant bath temperature	20±1 °C
Air gap distance	10 cm (dry/wet)

ing for performance evaluation.

4. Membrane Characterizations

4-1. Contact Angle Measurement

The hydrophilicity of the membranes was measured by the angle between the membrane surface and the meniscus formed by the water using a contact angle analyzer (Dataphysics, OCA 15Pro). The average of at least five measurements was reported.

4-2. Membrane Porosity and Pore Size Measurement

The membrane porosity was defined as the volume of the pores divided by the total volume of the porous membrane [40]. To measure the porosity, the membrane fibers were soaked and stored in deionized water for 24 h. Later, the fibers were weighed after wiping the excessive water on the membrane. It was followed by drying in a vacuum oven at 80 °C for 24 h before the mass of dry membrane was weighed again [39]. The porosity (ε) of each membrane was calculated using Eq. (1) [40]:

$$\varepsilon(\%) = \frac{(W_w - W_d)/D_w}{(w_w - w_d/D_w) + \left(\frac{W_d}{D_p}\right)} \times 100 \quad (1)$$

where W_w is the wet sample weight (g), W_d is the dry sample weight (g), D_w (0.998 g/cm^3) and D_p (0.37 g/cm^3) is the density of the water and polymer, respectively. Three samples for each membrane were measured and the averaged value was reported. Mean pore radius r_m (μm) was determined by filtration. According to Guerout Elford-Ferry equation, r_m was calculated as follows [39]:

$$r_m = \sqrt{\frac{(2.9 - 1.75\varepsilon) \times 8\eta l Q}{\varepsilon \times A \times \Delta P}} \quad (2)$$

where ε is the porosity of membrane (%), η is the water viscosity (8.9×10^{-4} Pa·s), l is the membrane thickness (m), Q is the volume of the permeate water per unit time (m^3/s), A is the effective area of the membrane (m^2) and ΔP is the trans-membrane pressure (Pa).

4-3. Scanning Electron Microscopy (SEM) and Energy Dispersive X-ray (EDX) Analysis

The morphology of membrane was characterized by Tabletop SEM (TM300, Hitachi). The samples of the membranes were first frozen in liquid nitrogen and then fractured. Cross-section and surface of the membranes were sputtered with platinum and then transferred to the microscope. The quality of dispersion and also the existence of SiO_2 on the membrane surface were assessed by EDX (QUANTAX 70, Bruker).

4-4. Fourier Transform Infrared Spectroscopy (FTIR)

The surface functionalization of SiO_2 nanoparticles with membrane was examined by using Fourier transform infrared spectroscope (FTIR, NICOLET 5700 FT-IR, Thermo Electron Corporation) recorded in the range of 800-1,800 cm^{-1} by the attenuated total refection (ATR) technique.

4-5. Thermal Analysis

The thermal stability and weight loss in the membranes was determined using TGA/SDTA 851^e analyzer (Mettler Toledo) that was carried out at a heating rate of 10 °C/ min up to 1,000 °C under air atmosphere.

4-6. Molecular Weight Cut-off

The molecular weight cut-off (MWCO) of membranes was characterized by measuring the rejection of PVP at different molecular weights (10, 40 and 360 g/mol). The concentration of PVP solution was prepared in 1 g/L for each test. A total organic carbon analyzer (TOC-LCPN, Shimadzu) was used to measure the amount of organic carbon in the permeate for the purpose of calculating the rejection of each membrane.

4-7. Filtration Experiments

The membrane performance was evaluated by the filtration and rejection experiments using a lab-scale permeation test rig. Tests were conducted to measure pure water flux, flux recovery and BSA separation of the control PES membrane and the PES/SiO_2 membranes using a cross flow system. All membrane samples were precompacted at 300 kPa using distilled water as feed for 1 h before any measurement was taken. The pure water flux of each membrane was then measured at pressure of 100 kPa by determining the volume of permeate collected at time intervals of 10 min.

$$J_w = V/At \quad (3)$$

where J_w is the water flux (L/m^2 h), V is the permeate volume (L), A is the membrane area (m^2) and t is the time (h).

Solute rejection was measured at 200 kPa in the same apparatus with aqueous solutions of BSA prepared by distilled water with the volume of 1,000 mL. The concentration of BSA solution is 1,000 mg/L. The BSA concentration in the feed and permeate samples was determined at the wave length of 280 nm using UV-Vis spectrophotometer (DR5000, Hach). Membrane cleaning was conducted by circulating the test rig with distilled water for 30 min. It was followed by re-measuring the flux of the membrane to determine

flux recovery rate (FRR). Rejection and FRR were calculated by Eq. (4) and (5), respectively.

$$R(\%)=\left(1-\frac{C_p}{C_f}\right)\times 100 \quad (4)$$

where C_p is the concentration of permeate and C_f is the concentration of feed in mg/L.

$$FRR\ (\%)=J_c/J_0\times 100 \quad (5)$$

where J_0 and J_c are the pure water flux ($L/m^2\cdot h$) of membrane before and after cleaning, respectively.

Fouling behavior can be demonstrated by the estimation of membrane resistance (m^{-1}) as follows:

Intrinsic membrane resistance (R_m)

$$R_m=\frac{TMP}{\mu\times J_0} \quad (6)$$

Total membrane resistance (R_t)

$$R_t=\frac{TMP}{\mu\times J_c} \quad (7)$$

Fouling resistance (R_f)

$$R_f=R_t-R_m \quad (8)$$

where TMP is trans-membrane pressure (kPa) and μ is permeate viscosity (mPa·s).

RESULTS AND DISCUSSION

1. Water Characterization

Table 2 shows the quality of water samples collected from WTP and PES/SiO_2 UF treated water together with the Malaysia water standard. The water quality of the treated water was found to comply the limit of the water standard for drinking purposes regulated by a local water company - Syarikat Air Johor (SAJ), Malaysia. These show that the application of PES/SiO_2 UF membrane was successful not only in removing metals and other organic compounds but also capable of eliminating bacterial colonies in the water sample.

2. Membrane Surface Morphology

The morphologies of the membrane surface and cross section were observed with SEM and the results are shown in Fig. 3 and 4, respectively. The membrane morphology consisted of a skin layer supported by porous layer of finger-like structures and macrovoids. The addition of SiO_2 had increased the outer skin layer thickness and the connectivity of the porous structure, leading to development of longer finger-like morphology in comparison with the control PES membrane (Fig. 3(a)). As can be seen from Fig. 3(b) and (c), the addition of SiO_2 in the polymeric solution had enlarged the microvoids of the membranes prepared. The change in membrane morphology is due to the fast exchange rate of solvent and non-solvent during phase inversion process [39]. For the membrane made of 4 wt% SiO_2 (Fig. 3(d)), the microvoids were significantly suppressed by the formation of longer finger-like structure and a relatively thick skin layer was formed. This could be due to the increase in dope solution viscosity upon addition of excessive SiO_2 content [25]. Higher dope solution concentration was reported to produce membranes with thicker and denser skin-layer, resulting in low porosity [43].

The skin layer surface of membranes in Fig. 4 showed the dispersion quality of SiO_2 on the membrane outer surface. The white objects spotted over the membrane surface indicated the presence of the SiO_2 nanoparticles. It can be seen that SiO_2 nanoparticles were detected across the surface of membranes made of 1 to 4 wt% SiO_2. However, SiO_2 nanoparticles formed significant agglomeration in the case where the membrane was made of 4 wt% SiO_2. This could be caused by nuclei of the polymer-poor phase formed during phase inversion process. The hydrophilic SiO_2 particles tend to migrate from the blended solution to the nuclei of the polymer-poor phase as it has more water than the surrounding blended solution. When the blended solution solidified, SiO_2 nanoparticles aggregated and stayed in some nuclei, which caused the formation of the agglomerate nanoparticles [40].

3. EDX Analysis

The EDX analysis investigated the elemental composition of SiO_2 nanoparticles on the membrane structure, and the results are shown

Table 2. The water quality parameters of untreated water samples and treated water by UF membrane prepared in this study

Water quality	Water samples from WTP	Treated water by PES/SiO_2 UF membrane	SAJ water standard requirement
pH	6.74	6.7	6.5-7.8
DO (mg/L)	6.7	8.11	-
Temp (°C)	25	25.9	-
Turbidity (NTU)	0.88	0.53	4.5
Colour	18.5	11	13.5
TOC (mg/L)	3.64	2.77	-
DOC (mg/L)	4.72	3.51	-
COD (mg/L)	10	3	-
Ammonia nitrogen, NH_4 (mg/L)	0.08	0.06	1.35
Iron, Fe (mg/L)	0.21	0.09	0.27
Aluminium, Al^{3+} (mg/L)	0.1	0.05	0.07
Manganese (mg/L)	0.05	0.04	0.09
Total bacterial count (ml^{-1})	22	0	-

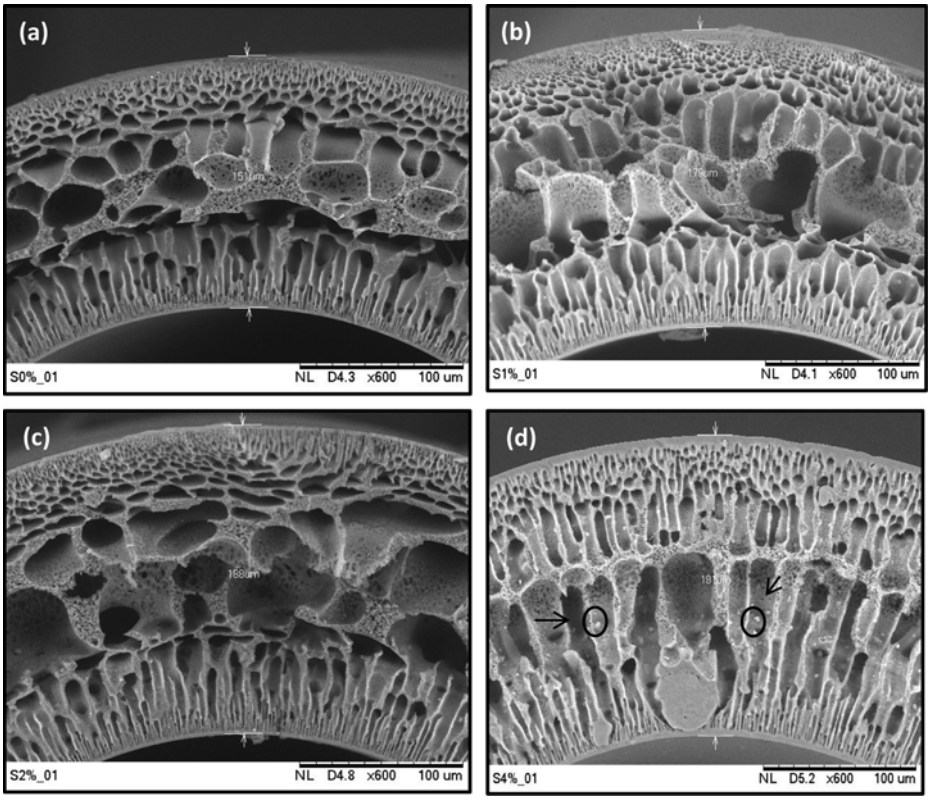

Fig. 3. Cross-sectional morphologies (scale bar: 100 μm) of the PES/SiO_2 membranes with (a) 0, (b) 1, (c) 2 and (d) 4 wt% SiO_2.

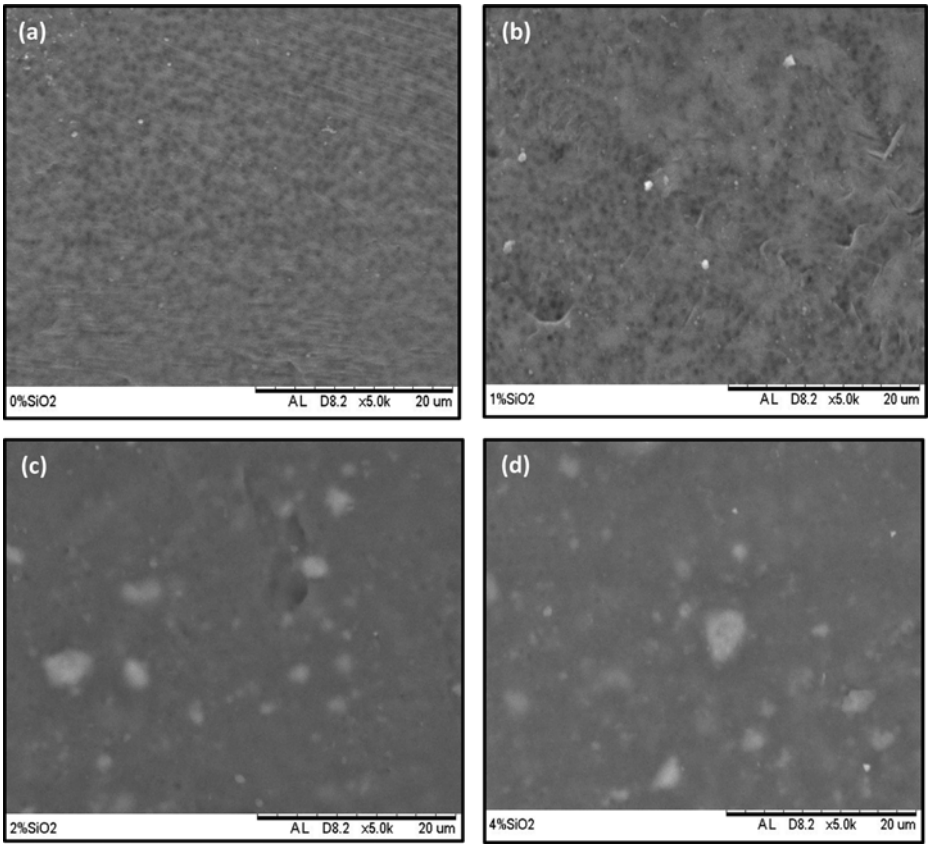

Fig. 4. Skin layer of outer surface morphologies (scale bar: 20 μm) of the PES/SiO_2 membranes with (a) 0, (b) 1, (c) 2 and (d) 4 wt% SiO_2.

Table 3. EDX analysis results of elemental composition in membranes (in atomic percentage)

Sample	C%	O%	S%	N%	Si%
Control PES	69.29	21.71	3.43	5.56	-
PES/1% SiO_2	67.21	23.17	4.05	5.55	0.03
PES/2% SiO_2	66.72	24.09	3.12	5.62	0.45
PES/4% SiO_2	67.17	22.71	2.93	6.50	0.68

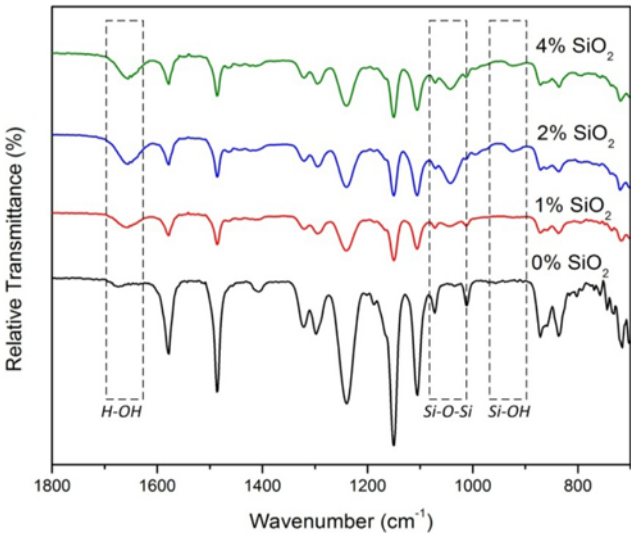

Fig. 5. FTIR spectra of control PES and PES/SiO_2 composite membranes with different SiO_2 loadings.

in Table 3. The control PES membrane contained significant quantities for sulfur, oxygen, carbon and nitrogen element but not silica. While for PES/SiO_2 composite membranes, additional signal of silica was found in which the higher the loading of SiO_2 added, the greater the amount of Si element was detected. These results confirm the incorporation of silica in the membrane with the highest silica content being in the PES membrane incorporated with 4 wt% SiO_2.

4. FTIR Analysis of SiO_2 Nanoparticles

The surface chemistry of control and PES/SiO_2 composite membranes was further investigated by FTIR, and the results are shown in Fig. 5. From the figure, the absorption band at 925 cm^{-1} is ascribed to Si-OH stretching. The broad H-O-H peaks observed at around 1,656 cm^{-1} indicate a major contribution from Si-OH or -OH groups of the polymer solution and the absorption band at 1,042 cm^{-1} is the asymmetrical stretch vibration absorption of Si-O-Si [39]. These absorption peaks indicate that SiO_2 particles were successfully incorporated into the membrane matrix.

5. Thermal Stability of the Membranes

Fig. 6 presents the TGA results of control PES and PES/SiO_2 composite membranes. The TGA curve shows two major weight loss regions. The first region, which is the minimum weight loss between 50 and 200 °C as observed for all membranes, is due to the loss of the adsorbed water, glycerol and the residual DMAC solvent (boiling point: 165 °C) from the membranes. The second region weight loss which occurs for 200-550 °C is due to the PES polymer that

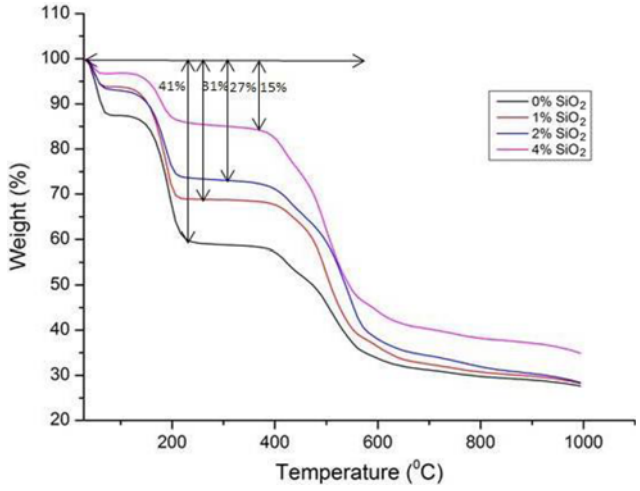

Fig. 6. TGA for control PES and PES/SiO_2 composite membranes.

has a decomposition temperature between 350 °C and 500 °C [34]. The weight loss was recorded at about 41, 31, 27 and 15% for the membrane incorporated with zero, 1, 2, and 4 wt% SiO_2, respectively. The degradation peaks of PES/SiO_2 membranes which shifted toward higher temperatures suggested the improved thermal stability of the composite membranes upon incorporation of SiO_2. This is because the presence of SiO_2 in the membrane tends to strengthen the interaction or chemical bonding between polymer matrix and silica networks of the membranes, contributing to the enhancement of the thermal stabilities [44]. In addition, SiO_2 is also reported to be able to improve mass transport barrier effects to the oxidizing atmosphere and the volatile compounds generated during degradation [40]. The interaction between SiO_2 nanoparticles and PES tends to increase the rigidity of polymer chain that consequently enhances the energy required for breaking down of polymer chain [45].

6. Molecular Weight Cut-off (MWCO)

The MWCO of a membrane corresponds to the smallest molecular weight of solutes that has the rejection of 90% [40]. The MWCO for each membrane sample in this study is shown in Fig. 7. The

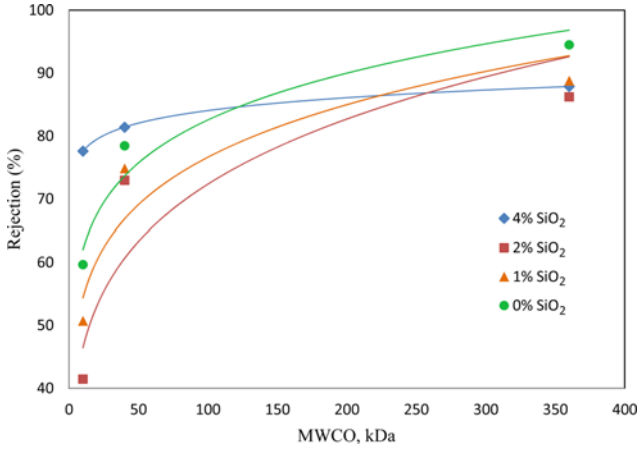

Fig. 7. Molecular weighs cut-off for control PES and PES/SiO_2 membranes.

MWCO for PES membrane incorporated with zero, 1 and 2 wt% SiO_2 is approximately 200, 300 and 310 kDa, respectively. The PES membrane incorporated with highest nanoparticle loading exhibited the highest MWCO, i.e >360 kDa. This indicates that the integration of SiO_2 nanoparticles in polymer solution would alter the MWCO of the membranes, resulting in larger surface pore size formation. Similar findings were also reported by Arthanareeswaran et al. [46], in which the addition of SiO_2 led to the increasing membrane MWCO. According to the authors, the increase of MWCO in the blend membranes may be due to the increase in free volume and a decrease in polymer chain segmental mobility by the presence of silica in the dope solution.

7. Flux and Rejection Performance of Membranes

Contact angle was used to measure the hydrophilicity of membrane by shape analysis in a three-phase system which consisted of the membrane surface, air and a drop of water [11]. The measurement was conducted five times on different locations of same membrane sample, and the average values are shown in Table 4. The addition of SiO_2 content has resulted in lower membrane contact angles, even though the membranes are within a narrow range of 77.9° to 71.0°. The contact angle of control PES membrane (77.9°) was decreased to 73.9° with the introduction of 2 wt% SiO_2, which indicates the better hydrophilic properties of composite membrane compared with the pure PES membrane. The increase of SiO_2 content in the dope solution will increase membrane pore size, porosity, and hydrophilicity, which leads to the enhancement of water flux. This is because the addition of SiO_2 nanoparticles will cause the instantaneous demixing during the phase inversion process that will eventually form porous structure in membranes [47]. Apart from that, the improvement of hydrophilic properties in membrane will lead to the increase of water flux because hydrophilic membranes are strongly attracted to water that will hinder unwanted solutes from adhering at the membrane surface [24].

The membrane performance was measured with respect to pure water flux and BSA rejection. Table 4 shows the results of the membrane pure water flux, while Fig. 8 shows the membrane water flux profile as a function of time. The highest water flux was found in the membrane incorporated with 2 wt% SiO_2 (87.23 L/m^2·h), and the lowest water flux was by the control PES membrane (44.16 L/m^2·h). Compared to the control membrane, the water flux of 2 wt% SiO_2 membrane was increased almost two-fold. Further increase in SiO_2 content from 2 to 4 wt%, however, negatively affected water flux. This is because the relatively thick skin layer of the membrane made of 4 wt% SiO_2 as evidenced from SEM image (Fig. 3(d)) causes the transport resistance of water molecules to increase.

The BSA rejection test and porosity of each membrane are shown in Fig. 9. The results show that the BSA rejection for the PES/SiO_2 membranes was higher compared to the control PES membrane. The highest rejection of 93.6% was achieved by 2 wt% SiO_2 membrane followed by 4 and 1 wt% membranes with 89.5% and 85.7% rejection, respectively. Meanwhile, the control PES membrane only exhibited around 80% rejection. These results suggest that there is a significant influence of SiO_2 content on the rejection capability of a membrane. In addition to the separation based on sieve effect mechanism, the adsorption mechanism of a membrane incorporated with SiO_2 nanoparticles should also be taken into consideration. As SiO_2 nanoparticles contain silanol groups that have high adsorption capacity for contaminants [48], the addition of SiO_2 in the polymer matrices will increase the silanol (Si-OH) and siloxane (Si-O-Si) bonding groups as shown in Fig. 5 (FTIR analysis). These bonding groups could act as adsorption sites for adsorbates at the membrane surface [49]. It is highly possible for BSA to interact with two or more silanol groups and adsorb to the membrane surface [50]. Thus, the increase of SiO_2 in the polymer solution will increase the adsorption mechanism in the membrane and enhance the separation performance. Fig. 9 also shows that the increase of porosity in the PES/SiO_2 membranes did not affect the BSA rejec-

Table 4. Performance of control PES and PES-SiO_2 membranes with different SiO_2 contents

SiO_2 content (wt%)	Contact angle (°)	Porosity (%)	Pore size (μm)	Pure water flux (L/m^2·h)
0	77.9±0.3	54.0	0.0917	44.16
1	74.9±0.5	61.5	0.0920	65.86
2	73.9±0.3	63.8	0.0937	87.23
4	71.0±0.4	62.7	0.0977	69.43

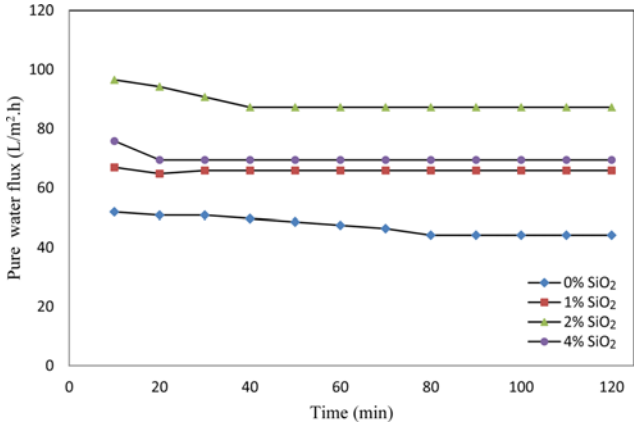

Fig. 8. Pure water flux of control PES and PES/SiO_2 composite membranes as a function of filtration time.

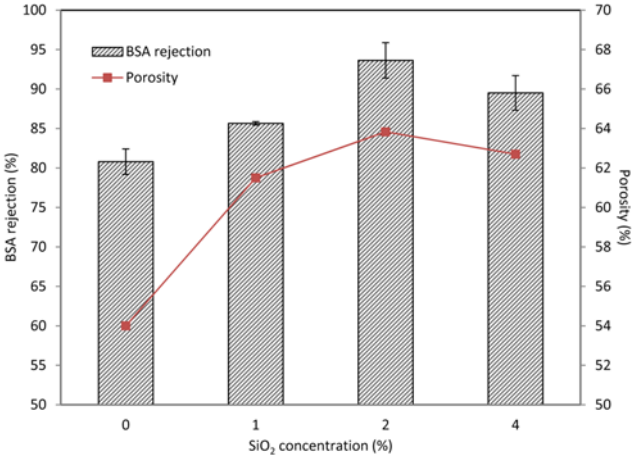

Fig. 9. The BSA rejection and porosity of control PES and PES/SiO_2 membranes.

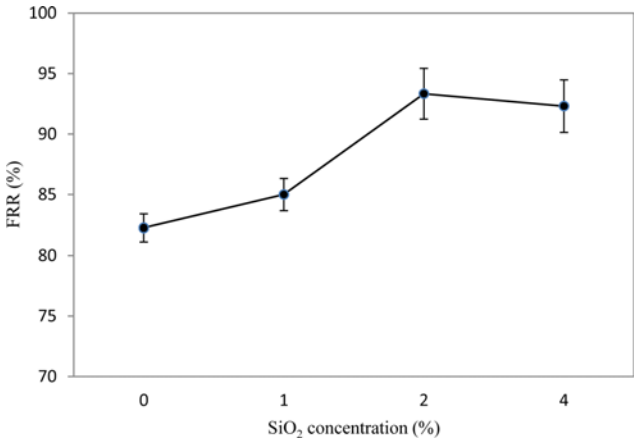

Fig. 10. The flux recovery rate (FRR) of control PES and PES/SiO_2 membranes.

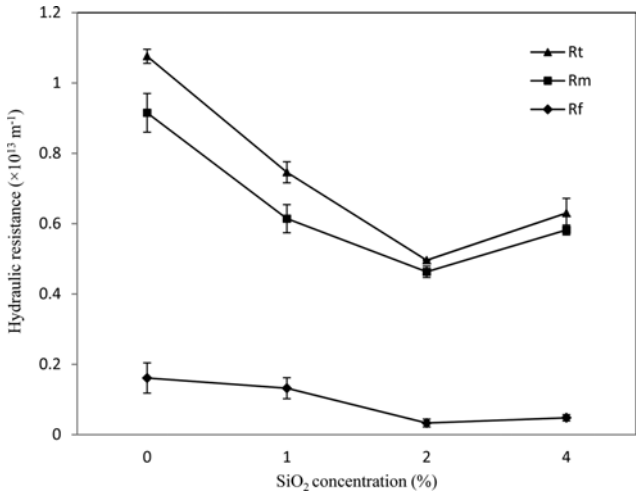

Fig. 11. The hydraulic resistance of control PES and PES/SiO_2 composite membranes.

tion. This is likely because the increase in the membrane porosity is balanced with the compact structure of the organic-inorganic network [36]. Hence, PES/SiO_2 membranes have greater permeability and rejection compared to the control PES membrane.

8. Anti-fouling Performance

The water sample from the WTP was pre-treated samples which may contain wide variety of micro-molecules that are prone to membrane fouling. These include bacteria, viruses, organic and inorganic compounds. Fouling in membrane can decrease the permeation efficiency and limit the widespread of UF membrane application. Therefore, membrane is usually cleaned to recover water flux [51]. The anti-fouling performance of the control and PES/SiO_2 composite membranes was analyzed by measuring the water flux recovery rate (FRR) and hydraulic resistance of membranes. The FRR results of the PES and PES/SiO_2 membrane with different SiO_2 content after cleaning process are shown in Fig. 10. Higher FRR was observed for the membranes modified by SiO_2 compared to the control PES membrane after both types of membranes were subjected to the same cleaning method. The FRR was recorded at 82.3% and 85% for the control PES and the membrane with 1 wt% SiO_2, respectively. The FRR was further increased to the highest value of 93.3% as shown in with 2 wt% SiO_2 before decreasing to 92.3% in the membrane of 4 wt% SiO_2. Since the PES/SiO_2 composite membranes exhibited better hydrophilic properties than the control membrane, the adsorption of micro molecules onto the membrane surface was expected to be lower and a simple water washing was considered effective to recover membrane water flux.

The hydraulic resistances that were measured in this study included intrinsic (R_m), fouling (R_f) and total (R_t) resistance. The intrinsic resistance refers to the pure water resistance of the membrane itself, while fouling resistance is the resistance that occurs due to the pore blocking on membrane surface [52,53]. Salahi et al. [30] pointed out that the pore blocking in membrane can occur as standard pore blocking (inside of the pores), intermediate pore blocking, and complete pore blocking or cake/gel layer formation (outside of the pores). For this study, only standard pore blocking is considered, as the membrane pores are generally larger than the size of the particles present in the water samples. Fig. 11 compares the values of R_m, R_f and R_t of the four membranes studied. As can be seen, the R_f was lower than R_m, because the water samples used were pretreated samples from the water treatment plant, so the occurrence of fouling on the membrane surface is minimum. The R_m is higher due to the micro molecules that are easily adsorbed to the internal pore walls of membrane by attractive electrostatic forces and high solute concentrations [54]. This eventually leads to pore blocking of membrane and increase in hydraulic resistance. As a result, the total hydraulic resistance of control PES membrane was higher ($1.076\times1{,}013\ m^{-1}$) compared to PES membrane with 2 wt% SiO_2 ($0.496\times1{,}013\ m^{-1}$). These show that the hydraulic resistance in PES membrane with 2 wt% SiO_2 was significantly improved as SiO_2 nanoparticles played an important role in decreasing membrane fouling. The results of FRR and filtration resistance confirmed the greater anti-fouling performance of the PES/SiO_2 composite membrane prepared.

CONCLUSIONS

PES/SiO_2 composite membranes were successfully prepared by phase inversion method. The addition of SiO_2 in the dope solution could alter the properties of the membrane prepared. The main conclusions are as follows:

1. The morphology of the cross-section of membrane structure was affected by the addition of SiO_2. The apparent visual is the increase of the macrovoid formation for the membranes made of lower content of SiO_2 nanoparticles. However, excessive use of SiO_2 (4 wt%) tended to produce a membrane with thicker skin layer.

2. The EDX and FTIR results confirmed the successful incorporation of SiO_2 in the polymeric matrix as silicon (Si) element, and its functional group were detected from these analyses.

3. Results from TGA analysis showed that the thermal stability of the PES/SiO_2 composite membranes was significantly improved compared to the control PES membrane.

4. The hydrophilicity property of the PES membrane was improved upon addition of hydrophilic SiO_2 nanoparticles that led to higher pure water flux and greater BSA rejection.

5. Higher FFR was obtained in the PES/SiO_2 membranes compared to the control PES membrane used for filtration process of pre-treated water samples from WTP. The appropriate addition of SiO_2 content in membrane is found to improve membrane anti-fouling ability as the R_t value was lower.

6. The water quality parameters of the treated sample by PES/SiO_2 membrane showed that the membrane was capable of removing metals and other organic compounds in the water samples. The introduction of SiO_2 nanoparticles in the PES membrane making was promising in improving membrane structural characteristics and has the potential to be employed for advanced water treatment process of drinking water production.

ACKNOWLEDGEMENTS

The authors wish to thank Universiti Teknologi Malaysia and Ministry of Higher Education Malaysia for providing LRGS grant (R.J30000.7809.4L810) on Water Security entitled Protection of Drinking Water: Source Abstraction and Treatment (203/PKT/6720006) as financial support of this project. This support is greatly appreciated.

NOMENCLATURE

A : effective area of the membrane [m^2]
A : membrane area [m^2]
C_p : concentration of permeate [mg/L]
C_f : concentration of feed [mg/L]
D_w : density of the water [0.998 g/cm^3]
D_p : desnsity of polymer [0.37 g/cm^3]
FRR : flux recovery ratio [%]
J_w : water flux [L/m^2 h]
J_0 : pure water flux of membrane before cleaning [L/m^2 h]
J_c : pure water flux of membrane after cleaning [L/m^2 h]
l : membrane thickness [m]
Q : volume of the permeate water per unit time [m^3/s]
r_m : mean pore radius [μm]
R : rejection [%]
R_m : intrinsic membrane resistance [m^{-1}]
R_t : total membrane resistance [m^{-1}]
R_f : fouling resistance [m^{-1}]
t : time [h]
TMP : trans-membrane pressure [kPa]
V : permeate volume [l]
W_w : wet sample weight [g]
W_d : dry sample weight [g]
ρ : porosity of membrane [%]
η : water viscosity [8.9×10^{-4} Pa·s]
ΔP : trans-membrane pressure [Pa]
ε : membrane porosity [%]
μ : permeate viscosity [mPa·s]

REFERENCES

1. X. Qu, P. J. J. Alvarez and Q. Li, *Water Res.*, **47**, 3931 (2013).
2. C. Zhao, J. Xue, F. Ran and S. Sun, *Prog. Mater. Sci.*, **58**, 76 (2013).
3. J. P. Chen, H. Mou, L. K. Wang, T. Matsuura and Y. Wei, in *Handbook of Environmental Engineering*, L. K. Wang, J. P. Chen, Y.-T. Huang and N. K. Shammas Eds., Humana Press Inc. (2011).
4. J. Schrotter and B. Bozkaya-schrotter, in *Membrane Technology: Membranes for Water Treatment*, K.-V. Peinemann and S. P. Nunes Eds., Wiley-VCH Verlag GmbH & Co. KGaA, Weinheim, Germany (2010).
5. O. Ferrer, X. Serrallach, F. Horváth, J. Mesa, O. Gibert and X. Bernat, *Desalin. Water Treat.*, **51**, 1831 (2013).
6. H. P. Huq, J.-S. Yang and J.-W. Yang, *Desalination*, **204**, 335 (2007).
7. A. Teuler, À. Vega, J. Coma, D. Vidal and J. Aumatell, *Desalin. Water Treat.*, **51**, 140 (2013).
8. J. Guilbaud, A. Massé, F.-C. Wolff and P. Jaouen, *Desalin. Water Treat.*, **51**, 416 (2013).
9. D. B. Mosqueda-Jimenez and P. M. Huck, *Desalination*, **198**, 173 (2006).
10. Y. X. Yang and J. Chen, *Adv. Mater. Res.*, **647**, 543 (2013).
11. S. B. Teli, S. Molina, E. G. Calvo, A. E. Lozano and J. de Abajo, *Desalination*, **299**, 113 (2012).
12. B. Vatsha, J. C. Ngila and R. M. Moutloali, *Phys. Chem. Earth, Parts A/B/C*, **67**, 125 (2014).
13. J. P. Chen, H. Mou, L. K. Wang and T. Matsuura, in *Handbook of Environmental Engineering*, L. K. Wang, Y.-T. Hung and N. K. Shammas Eds., Humana Press Inc., Totowa, NJ (2006).
14. W. Gao, H. Liang, J. Ma, M. Han, Z. Chen, Z. Han and G. Li, *Desalination*, **272**, 1 (2011).
15. L. Fiksdal and T. Leiknes, *J. Membr. Sci.*, **279**, 364 (2006).
16. S. Xia, X. Li, R. Liu and G. Li, *Desalination*, **167**, 23 (2004).
17. E. Debik, G. Kaykioglu, A. Coban and I. Koyuncu, *Desalination*, **256**, 174 (2010).
18. C. Fersi and M. Dhahbi, *Desalination*, **222**, 263 (2008).
19. K. Chon, S. J. Kim, J. Moon and J. Cho, *Water Res.*, **46**, 1803 (2012).
20. H.-H. Cheng, S.-S. Chen and S.-R. Yang, *Sep. Purif. Technol.*, **70**, 112 (2009).
21. S. Nakatsuka, I. Nakate and T. Miyano, *Desalination*, **106**, 55 (1996).
22. K. Hagen, *Desalination*, **119**, 85 (1998).
23. P. S. Goh, B. C. Ng, W. J. Lau and A. F. Ismail, *Sep. Purif. Rev.*, **44**, 216 (2014).
24. A. L. Ahmad, A. A. Abdulkarim, B. S. Ooi and S. Ismail, *Chem. Eng. J.*, **223**, 246 (2013).
25. B. S. Lalia, V. Kochkodan, R. Hashaikeh and N. Hilal, *Desalination*, **326**, 77 (2013).
26. A. Ananth, G. Arthanareeswaran and H. Wang, *Desalination*, **287**, 61 (2012).
27. H. Adib, S. Hassanajili, M. R. Sheikhi-Kouhsar, A. Salahi and T. Mohammadi, *Korean J. Chem. Eng.*, **32**, 159 (2015).
28. L. Y. Ng, A. W. Mohammad, C. P. Leo and N. Hilal, *Desalination*, **308**, 15 (2013).
29. J. Kim and B. Van der Bruggen, *Environ. Pollut.*, **158**, 2335 (2010).
30. A. Salahi, T. Mohammadi, R. M. Behbahani and M. Hemmati, *Korean J. Chem. Eng.*, **32**, 1 (2015).
31. H. Basri, A. F. Ismail and M. Aziz, *Desalination*, **273**, 72 (2011).
32. L. Yan, Y. Li, C. Xiang and S. Xianda, *J. Memb. Sci.*, **276**, 162 (2006).
33. R. Pang, X. Li, J. Li, Z. Lu, X. Sun and L. Wang, *Desalination*, **332**, 60 (2014).
34. A. Razmjou, A. Resosudarmo, R. L. Holmes, H. Li, J. Mansouri and V. Chen, *Desalination*, **287**, 271 (2012).

35. A. Idris, I. Ahmed and M. A. Limin, *Desalination*, **250**, 805 (2010).
36. J. Shen, H. Ruan, L. Wu and C. Gao, *Chem. Eng. J.*, **168**, 1272 (2011).
37. M. Sun, Y. Su, C. Mu and Z. Jiang, *Ind. Eng. Chem. Res.*, **49**, 790 (2010).
38. W.-Z. Lang, J.-P. Shen, Y.-X. Zhang, Y.-H. Yu, Y.-J. Guo and C.-X. Liu, *J. Memb. Sci.*, **430**, 1 (2013).
39. H. Yu, X. Zhang, Y. Zhang, J. Liu and H. Zhang, *Desalination*, **326**, 69 (2013).
40. J. Huang, K. Zhang, K. Wang, Z. Xie, B. Ladewig and H. Wang, *J. Membr. Sci.*, **423**, 362 (2012).
41. S. Kango, S. Kalia, A. Celli, J. Njuguna, Y. Habibi and R. Kumar, *Prog. Polym. Sci.*, **38**, 1232 (2013).
42. P. Christian, in *Environmental and Human Health Impacts of Nanotechnology,* J. R. Lead and E. Smith Eds., Blackwell Publishing Ltd. (2009).
43. N. A. A. Sani, W. J. Lau and A. F. Ismail, *Korean J. Chem. Eng.*, **31**, 1 (2015).
44. L.-Y. Yu, Z.-L. Xu, H.-M. Shen and H. Yang, *J. Membr. Sci.*, **337**, 257 (2009).
45. J. Liu, Y. Li, X. Wang, Q. Zhang and J. Yang, *J. Macromol. Sci., Part B Phys.*, **50**, 2356 (2011).
46. G. Arthanareeswaran, T. Sriyamunadevi and M. Raajenthiren, *Sep. Purif. Technol.*, **64**, 38 (2008).
47. G. R. Guillen, Y. Pan, M. Li and E. M. V Hoek, *Ind. Eng. Chem. Res.*, **50**, 3798 (2011).
48. S. Rasalingam, R. Peng and R. T. Koodali, *J. Nanomater.*, **2014**, 1 (2014).
49. I. Turku, T. Sainio and E. Paatero, *Environ. Chem. Lett.*, **5**, 225 (2007).
50. J. A. Velasco, F. Rojas and V. H. Lara, *Ind. Eng. Chem. Res.*, **43**, 1779 (2004).
51. P. Kanagaraj, S. Neelakandan and A. Nagendran, *Korean J. Chem. Eng.*, **31**, 1057 (2014).
52. T.-H. Bae and T.-M. Tak, *J. Membr. Sci.*, **249**, 1 (2005).
53. S.-J. Lee, M. Dilaver, P.-K. Park and J.-H. Kim, *J. Membr. Sci.*, **432**, 97 (2013).
54. R.-S. Juang, H.-L. Chen and Y.-S. Chen, *Sep. Purif. Technol.*, **63**, 531 (2008).